COMPARISON OF COMBUSTION DEPOSITS FROM BITUMINOUS COALS AND A LIGNITE

F. E. Huggins[1], G. P. Huffman[2],

Departments of Geological Sciences[1] and Chemical Engineering[2],
University of Kentucky,
Lexington, KY 40506

and A. A. Levasseur

Kreisinger Development Laboratory,
Combustion Engineering, Inc.,
P.O. Box 500,
Windsor, CT 06095

INTRODUCTION

Deposits generated during combustion of pulverized coals are determined to a large extent by the type, relative amounts, size, and association of the different inorganic species present in the coal. In this investigation, we examine and compare the inorganic constituents in various samples of two bituminous coals and of a Texas lignite and the deposits generated from these coals in the same test furnace. Whereas the principal basic mineral in the bituminous coals is pyrite, which is found in these coals in relatively coarse particle form, the principal component in the lignite is carboxyl-bound calcium, which is highly dispersed throughout the lignite macerals. These situations can be considered to represent different ends of the spectrum with respect to the size and distribution of the major basic component of the inorganic species.

The mineral matter of the coals was characterized using a combination of computer-controlled SEM (CCSEM) and Mössbauer spectroscopic methods. Similar techniques were used to examine deposits.

EXPERIMENTAL

(a) Samples:

The Illinois #6 coal was obtained as a combustion product (Il#6-Base) and as a cleaned metallurgical product (Il#6 - Met). The other two coals, a Kentucky #9 coal and a Texas Lignite, were subjected to cleaning at the EPRI Coal Cleaning Test Facility, near Homer City, PA. A medium-cleaned product (Ky#9 - MCln) and a deep-cleaned product (Ky#9 - DCln) were prepared from the original Kentucky #9 coal (Ky#9-Raw) and a cleaned product (TexL - Cln) was prepared from the original lignite (TexL - Raw). Pulverized coal samples were prepared from the original coals and the cleaned products. These coals were then burnt in the Fireside Performance Test Facility (FPTF) at Combustion Engineering and a variety of deposit samples were collected, including in-flame solids, superheater deposits and waterwall deposits.

(b) Techniques:

The combination of Mössbauer spectroscopy and CCSEM for the determination of coal mineralogies has been described in detail elsewhere (1). Basically, the CCSEM technique determines quantitatively the types, relative amounts, and size distributions of the major discrete minerals in the coal, whereas Mössbauer spectroscopy provides more detailed complementary information regarding the iron-bearing minerals, in particular pyrite. For lignites, however, the CCSEM method does not determine the carboxyl-bound inorganics dispersed in the lignite macerals. These components were semi-quantitatively

estimated from a comparison of the discrete mineralogy and the overall inorganic composition as revealed by wide area energy dispersive X-ray scans or the chemical analysis of the high-temperature ash.

For samples generated in the FPTF, Mössbauer spectroscopy was used to document the behavior of iron in the various deposits and optical and electron microscopic techniques were used to examine the microstructure and mineralogy in polished sections of the deposit mounted in epoxy. Much reliance was placed on elemental X-ray and backscattered electron intensity mapping techniques in the CCSEM to document element distributions and associations.

Some exploratory extended X-ray absorption fine-structure (EXAFS) spectroscopy measurements were made at the calcium K-edge to investigate the form of occurrence of Ca in the Texas lignite and Illinois #6 coal and in deposits generated from the coals. These measurements will be discussed in detail elsewhere and will merely be mentioned here in passing where information from the EXAFS technique corroborates or supplements data from the other techniques.

RESULTS

(a) Coal Mineralogies:

The mineralogies of the various coal samples are summarized in Table 1. The samples from the Illinois #6 and Kentucky #9 bituminous coals exhibit somewhat similar mineralogies: pyrite, along with its oxidation products, is the principal basic mineral, although both raw coals also contain significant amounts of calcium minerals: gypsum in Kentucky #9, calcite in Illinois #6. However, the combination of quartz and clay minerals dominates the mineralogies. The Texas lignite discrete mineralogy is dominated by quartz; pyrite and other basic minerals are very minor components. Cleaning does effect some differences in mineralogy: both bituminous coals become relatively poorer in pyrite with cleaning. However, for the Kentucky #9 coals, the decrease in pyrite is compensated by an increase in magnetite, which was introduced into the cleaned coals from the heavy media used for cleaning. This contamination is best revealed by the Mössbauer data and spectrum (Fig. 1). The discrete mineralogy of the Texas lignite is little affected by cleaning; however, the ratio of the discrete mineral matter to the dispersed maceral inorganics changes from approximately 2:1 to less than 1:1 based on changes in the overall energy-dispersive X-ray composition. The major dispersed inorganic elements were calcium and sulfur. EXAFS spectroscopy confirmed that calcium was present as carboxyl-bound Ca in macerals, based on the similarity of the Ca EXAFS spectrum to previously published data on Ca in lignites (2).

Some data are presented on mineral size distributions in Table 2. As can be seen from Table 2 and more clearly for the Kentucky #9 coals shown plotted on a wt% coal basis in Fig. 2, cleaning has the effect of preferentially removing the coarser mineral matter (>20μm). Hence, specific minerals with a coarser size distribution are removed more completely than those with size distributions biased to smaller size ranges. It is clear that the relative size distributions explains why pyrite and not quartz is removed by the cleaning of the Kentucky #9 coal. Although less dramatic, there is also a significant reduction in the coarse quartz content of the Texas lignite upon cleaning; however, there is little change in the discrete mineralogy (Table 1), implying that all minerals are, on average, similarly affected.

It should be noted, however, that cleaning reduces the basic mineral content of the bituminous coals, but increases the proportion of basic inorganics for the Texas lignite.

TABLE 1a: COAL MINERALOGIES BY CCSEM+

	Kentucky #9			Illinois #6		Texas Lignite	
Mineral	Raw	MCln	DCln	Base	Met.	Raw	Cln
Quartz	14	16	24	17	20	47	36
Kaolinite	2	4	5	8	9	3	12
Illite	3	6	9	10	17	3	3
Misc. Sil.	22	26	21	28	31	34	28
Pyrite	29	19	16	22	11	3	9
Gypsum	8	3	3	2	2	--	--
Fe sulfate	2	5	4	1	2	--	--
Misc. Sulf.	5	3	3	2	2	--	--
Fe-rich	1	6	6	<1	2	1	2
Ca-rich	--	--	--	8	<1	2	1
Misc., mixed	14	12	9	2	4	6	8

+Data expressed as percentage of mineral matter

TABLE 1b: MÖSSBAUER DATA ON DISTRIBUTION OF IRON

	Kentucky #9			Illinois #6		Texas Lignite	
%Fe in	Raw	MCln	DCln	Base	Met.	Raw	Cln
Pyrite	65	60	48	87	84	71*	67*
Clay	3	4	3	--	5	--	--
Szomolnokite	1	--	--	7	--	14	8
Jarosite	32	26	33	5	11	15*	25*
Magnetite	--	11	16	--	--	--	--
Wt% Pyr. S	1.30	0.81	0.34	1.05	0.48	0.32	0.17

*Absorptions are broad; may include minor FeOOH

(b) Deposits:

(i) In-flame Solids: The samples of in-flame solids collected from in or near the flame region during the burning of the bituminous coals consisted, for the most part, of very loose aggregates of fly-ash cenospheres. Compositions of the individual cenospheres as revealed by EDX spectra and CCSEM mapping were highly variable reflecting the different associations of minerals in the coal particles. As might be expected, the fly ash particles were smaller and more uniform in size for the cleaned coals compared to the raw coals. Occasionally, these aggregates had nuclei of more highly agglomerated material or of large pieces of incompletely burnt char. Iron in all the samples was distributed among glass (both ferric and ferrous components), magnetite, and minor hematite. No iron sulfide or crystalline iron silicate phase could be discerned from the Mössbauer spectra. Typically over 50% of the iron was present in glass and the cleaned lignite had the most Fe in this form, up to 90%. Extensive reaction between silicates and pyrite must occur very rapidly in the initial combustion process in the flame.

TABLE 2: MINERAL SIZE DISTRIBUTION DATA FOR COALS

Coal	Size Distribution Data - All Minerals					
	<2.5μm	2.5-5μm	5-10μm	10-20μm	20-40μm	>40μm
Ky#9 - Raw	20	14	21	25	14	7
- MCln	27	21	23	16	11	1
- DCln	27	29	26	12	4	2
Il#6 - Base	21	16	19	21	11	12
- Met.	30	17	22	17	6	7
TexL - Raw	21	7	13	14	21	23
- Cln	21	15	20	16	13	16

Coal	Size Distribution Data - Pyrite					
	<2.5μm	2.5-5μm	5-10μm	10-20μm	20-40μm	>40μm
Ky#9 - Raw	9	6	25	22	21	17
- MCln	10	15	24	21	30	0
- DCln	14	16	35	26	9	0
Il#6 - Base	9	6	18	31	20	16
- Met.	16	11	29	27	14	4
TexL - Raw	--	--	--	--	--	--
- Cln	--	--	--	--	--	--

Coal	Size Distribution Data - Quartz					
	<2.5μm	2.5-5μm	5-10μm	10-20μm	20-40μm	>40μm
Ky#9 - Raw	15	22	33	24	4	3
- MCln	22	25	38	13	2	0
- DCln	17	31	36	8	2	6
Il#6 - Base	13	22	38	16	3	8
- Met.	21	18	24	13	1	24
TexL - Raw	10	5	10	13	31	31
- Cln	16	16	20	19	17	12

(ii)a Superheater Deposits - Initial: The initial superheater deposits from the bituminous coals are composed of largely undeformed silica and aluminosilicate cenospheres, less regular spherical particles rich in Fe and Si or Ca and S, and highly deformed Fe-rich particles. The latter particles often appear to be molded around the more rigid spheres, probably as a result of collision, and to be the "glue" that cements the deposit together. The interparticle contacts are quite sharp, indicating that little, if any, chemical reaction has taken place. Mössbauer data indicate a significant enrichment in iron by more than 50% for this type of deposit (Fig. 3), which also reinforces the importance of the iron particulate matter in the

cohesion of the deposit. In contrast to the in-flame solid samples, only 5-15% of the iron is present in glass, with the other 85-95% in the form of iron oxides, predominantly hematite.

Mössbauer data for the lignite superheater deposits, however, show no such enrichment in iron and less than 20% of the iron is present in magnetic oxides. For these deposits, iron does not appear to play a similar role to that in the bituminous coals. In this case the "glue" material may be calcium sulfate as this phase was shown by EXAFS spectroscopy to be very abundant in the initial deposit.

(ii)b Superheater Deposits - Outer: The structure of the outer superheater deposit is derived from the initial superheater structure by partial fusion and blending of the different fly-ash particulate matter. Many larger Fe-rich and Si-rich particles, however, persist unassimilated in the matrix so that the aluminosilicate particles become important at this stage as the major bonding phase. Partial fusion of these particles coupled with incorporation of all potassium and calcium phases and an appreciable fraction of the iron particles into this partial melt creates an extensive continuous framework. When frozen, these deposits were extremely tough and resistant to fracture because of this structure. For the bituminous deposits, Mössbauer data indicate that there is only a very minor enrichment of iron in these deposits compared to the in-flame solids and that there is a significantly higher percentage of iron in glass compared to the initial deposit.

The lignite outer superheater deposits varied from lightly sintered fly-ash to highly agglomerated amber-brown vitreous material. Fly-ash relicts, mostly large quartz particles and a few Fe-rich cenospheres, persist in less agglomerated areas and diminish in abundance with increasing agglomeration. The matrix is rich in calcium, aluminum and silicon and appears to have formed by reaction between Ca-rich and aluminosilicate particles. The matrix is quite highly crystallized with melilite ($Ca_2(Al,Mg,Fe,Si)_2SiO_7$) and anorthite ($CaAl_2Si_2O_8$) being the most common phases. Melilite tended to occur in the less agglomerated areas whereas anorthite was found in the more highly agglomerated areas.

(iii) Waterwall Deposits: An initial and outer waterwall deposit was collected for each coal. The initial deposit consisted of thin deposit whereas the outer deposit was considerably thicker and often collected in large masses. Mössbauer data showed some differences between the initial and outer deposits in that the initial deposits always contained more iron as oxides (except for the lignite), had a higher Fe^{3+}/Fe^{2+} ratio for the glass, and had less Al substituted for Fe in hematite, based on the magnetic hyperfine splitting parameter for this phase. However, there was little difference in the amount of iron between corresponding samples of waterwall deposit (Fig. 3).

The microstructure of the outer waterwall deposits from the bituminous coals varies significantly from the wallside to the fireside. At the immediate wallside is a thin layer that resembles the outer superheater deposit in that considerable fly-ash structure is present in a partially fused matrix. This layer is typically discontinuous towards the wall and offers a somewhat tenuous connection between the wall and the main body of the waterwall deposit. The continuous part of the deposit nearest the wallside exhibits a similar structure. Upon moving away from the wall, the relict Si-rich cenospheres are quickly assimilated into the matrix whereas the Fe-rich cenospheres fragment as the iron oxide equilibrates with the matrix. Upon moving further into the middle of the deposit, the Fe-rich fragments become increasingly angular and are eventually superseded by well crystallized, often skeletal, crystals of iron oxides. At the same time the glassy matrix becomes more

uniform in composition and appearance. On moving closer to the fireside, the iron oxides become less frequent and mullite laths begin to appear. At the immediate fireside, mullite occurs along with glass and the iron oxides occur as extremely fine scale dendrites. This latter phase probably developed upon cooling and was not present at temperature.

Similar microstructural changes are seen for the outer waterwall deposits from the lignite, but with different phases. In the adhesive layer, the fly-ash material is very calcium rich and contains appreciable sulfur and some Fe-rich particles. Large relict quartz particles are found near the wall and these appear to be only very slowly assimilated into the matrix. The matrix structure near the wall is fine-grained and chaotic, but coarsens considerably towards the center of the deposit as melilite crystallizes. Upon moving further towards the fireside, fewer quartz relicts are observed and the melilite crystallization is replaced by anorthite. In addition, crystallization of some minor phases such as calcium ferrites occurs in the outer waterwall samples.

For the raw Texas lignite sample, relict quartz was significantly more abundant than for the cleaned lignite sample. Furthermore, it appeared that the quartz was not so easily incorporated into the matrix of the raw lignite waterwall deposits. Occasionally, it was noted that a mantle of immiscible liquid was formed around the quartz particles that hindered the assimilation of this mineral into the Ca-rich matrix.

CONCLUSIONS

Despite significant differences in chemical composition, the microstructures of the lignite and bituminous deposits were quite similar and it would be difficult to identify a particular deposit as coming from a given coal in the absence of compositional information. However, this implies that similar structures can be brought about by quite different chemical interactions. In particular, the role of iron oxides in the initial formation of the superheater deposits and possibly also for the waterwall deposits from the bituminous coals is not evident for the lignite deposits. For these latter deposits, calcium sulfate may play a similar critical role, but this remains to be demonstrated. Partial fusion of the aluminosilicates accompanied by assimilation of basic cations into the matrix appears to be the principal cementing mechanism of both types of deposit, once they are established. As the deposits thicken and are subject to higher temperatures, the melts become more homogeneous and their mineralogy and behavior are largely governed by phase equilibria considerations.

In both types of deposits, relict Fe-rich and quartz fly-ash particles resist assimilation into the aluminosilicate matrix. In the case of the bituminous deposits, the abundance of iron oxide is such that it is either the liquidus phase or close to it. Hence, the aluminosilicate melts, except at very high temperatures, are effectively saturated with iron. In the case of the lignite deposits, quartz particles are generally quite large and assimilation in the melt is probably retarded because of sluggish reaction kinetics and also perhaps liquid immiscibility. This effectively makes the melt more basic than it should be and enables the crystallization of basic phases such as melilite. However, as quartz is absorbed into the melt and the composition becomes more acidic, anorthite takes over as the major crystallizing phase, as would be predicted from the CaO-Al_2O_3-SiO_2 phase equilibria diagram.

ACKNOWLEDGEMENTS

This work was supported by the Electric Power Research Institute by means of a contract to Combustion Engineering, Inc.

REFERENCES

(1) F.E. Huggins, G.P. Huffman, and R.J. Lee, in: Coal and Coal Products: Analytical Characterization Techniques, ACS Symposium Series 205 239-258, (1982).
(2) G.P. Huffman, and F.E. Huggins, in: Chemistry of Low-Rank Coals, ACS Symposium Series 264 158-174, (1984).

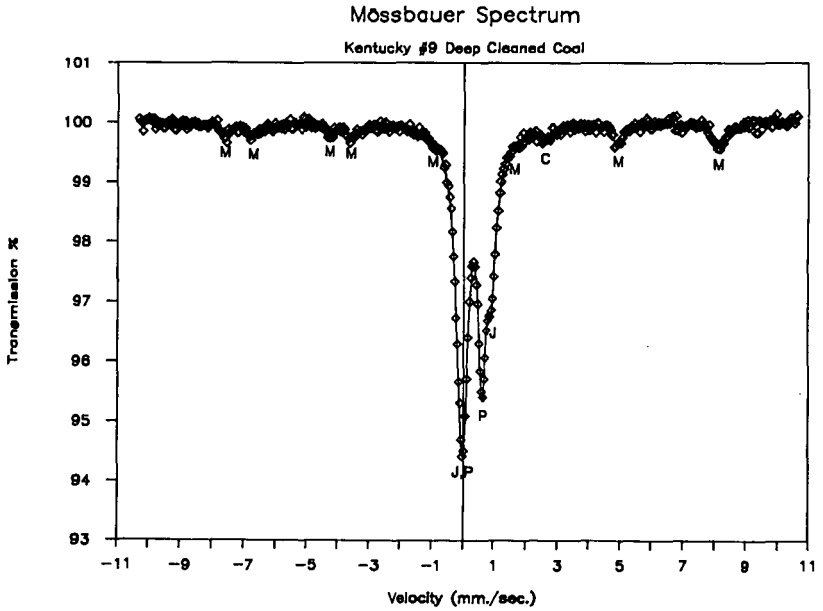

Figure 1: Mössbauer spectrum of the deep-cleaned Kentucky #9 coal showing the contamination by magnetite (M) from heavy-media cleaning. Other iron-bearing minerals present in the spectrum are pyrite (P), jarosite, (J) and ferrous-bearing clay (C).

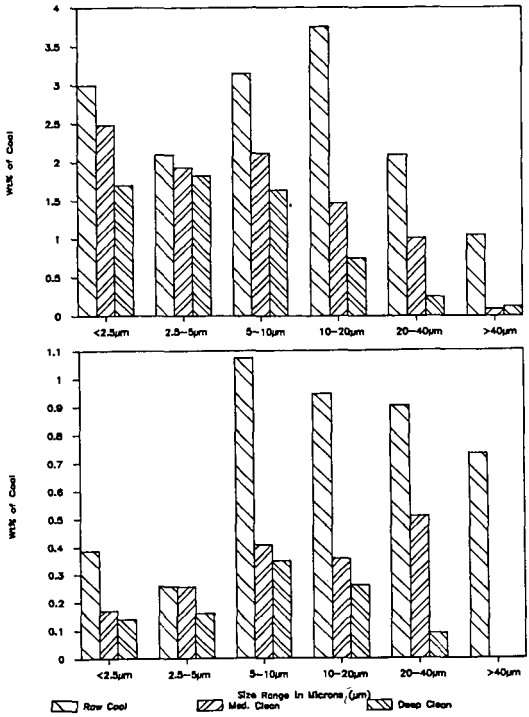

Figure 2: Size distribution data for all minerals (upper) and pyrite (lower) in Kentucky #9 coals. Data are expressed as wt% of the coal.

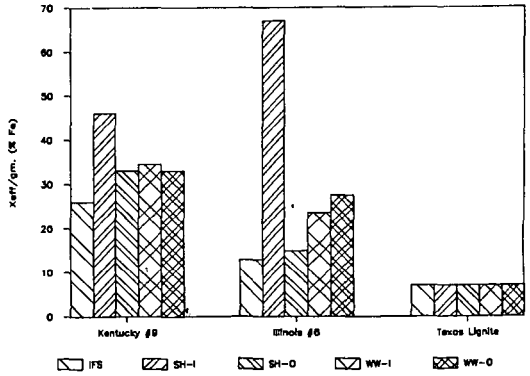

Figure 3: Histogram showing the significant enrichment in iron (based on the Mössbauer effective thickness parameter, X_{eff}/gm) for the initial superheater deposits from the raw bituminous coals and the lack of iron segregation exhibited by the lignite.
Key: IFS - in-flame solids; SH-I - initial superheater; SH-O - outer superheater; WW-I - initial waterwall; WW-O - outer waterwall.